

Micellar Ordering in Concentrated Solutions of Di- and Triblock Copolymers in a Slightly Selective Solvent

I. W. Hamley*

School of Chemistry and Centre for Self-Organising Molecular Systems, University of Leeds, Leeds, W. Yorkshire LS2 9JT, U.K.

J. P. A. Fairclough and A. J. Ryan

Manchester Materials Science Centre, UMIST, Grosvenor Street, Manchester M1 7HS, U.K.

C. Y. Ryu[†] and T. P. Lodge^{*,‡}

Departments of Chemistry and of Chemical Engineering and Materials Science, University of Minnesota, Minneapolis, Minnesota 55455

A. J. Gleeson

CLRC Daresbury Laboratory, Warrington, Cheshire WA4 4AD, U.K.

J. S. Pedersen

Department of Solid State Physics, Risø National Laboratory, Roskilde, DK-4000, Denmark

Received June 10, 1997; Revised Manuscript Received December 22, 1997

ABSTRACT: Micellar ordering in semidilute solutions of polystyrene–polyisoprene diblock and triblock copolymers in the slightly selective solvent di-*n*-butyl phthalate has been studied using rheology and small-angle X-ray scattering (SAXS). Ordering as a function of temperature has been investigated for a range of polymer concentrations $0.1 \leq \phi \leq 0.4$. For $\phi < 0.2$, the rheological response is liquidlike and SAXS shows that there is no intermicellar order in the liquid; however, the solution viscosity shows a strong maximum near 50 °C. Above a crossover concentration $\phi \approx 0.2$, ordering of micelles is indicated by the presence of a sharp structure factor peak. The ordered micellar structure, identified as hexagonal for $0.2 \leq \phi \leq 0.3$ and lamellar for $\phi \geq 0.3$, persists up to an order–disorder transition at $T \approx 40$ °C for the diblock and $T \approx 50$ °C for the triblock solutions studied. The rheological characteristics of the ordered solutions are reminiscent of those found in ordered block copolymer melts. At higher temperatures, for example approximately 20–30 °C above the ODT for the $\phi = 0.2$ solutions, indications of chain aggregation disappear from the rheological properties; however, some evidence of chain association persists to still higher temperatures in the SAXS profiles. The domain spacing, d , in the ordered solutions obtained from the principal structure factor peak position, shows a crossover at $\phi \approx 0.2$, in agreement with rheology. At high concentrations, d scales as $d \sim \phi^{-1/3}$, suggesting a three-dimensional contraction of the microstructure, and thus micelles of finite length. This concentration dependence is opposite to that previously observed for ordered block copolymer solutions in neutral solvents, due to the solvent selectivity. The results are gathered in a rather rich phase diagram for this system.

Introduction

Solutions of block copolymers are used extensively in the surfactant and cosmetics industries, and micellization in these solutions is of interest because it modifies the rheological properties of these commercial products. Although considerable attention has been paid to micellization in dilute solutions,¹ there has been less work on concentrated solutions.^{2–12} Similarly, the melt phase diagram of block copolymers has been studied extensively,¹³ but in concentrated solutions modifications to the melt phase diagram due to neutral or selective solvents have not been explored in detail. In this paper we examine nondilute block copolymer solutions, focusing on diblock and triblock copolymers in a solvent that is slightly selective for one of the blocks.

Block copolymers adopt a variety of ordered phases in the melt, due to unfavorable interactions between the

constituent monomers A and B. In dilute solution, unfavorable interactions between the solvent (S) and one of the monomers (B) can induce micellization. In semidilute and concentrated solutions one may therefore anticipate a rich phenomenology, as A–B, A–S, and B–S interactions all contribute to the free energy. In one limit, that of a neutral solvent, the diluted A–B interactions should drive self-assembly much as in the melt, but qualitative differences from meltlike behavior can still be found, such as in the scaling of the ordering concentration with chain length.⁹ In the other limit, that of a “strongly” selective solvent good for one block and a nonsolvent for the other, micellization should still occur as in dilute solution, but the micelles may be arranged on a lattice.¹⁴ For a solvent that is “slightly” selective, i.e., good for block A but close to the Θ temperature for block B, small changes in temperature can produce large changes in solution properties, as variations in temperature modulate the relative importance of B–S interactions.¹⁰

* Authors for correspondence.

[†] Department of Chemical Engineering and Materials Science.

[‡] Department of Chemistry.

Earlier work on nondilute block copolymer solutions has focused on swelling, where the scaling of the small-angle neutron scattering (SANS) or X-ray (SAXS) peak position with copolymer concentration was studied. Hashimoto and co-workers found that the domain spacing in the lamellar phase in concentrated solutions in neutral solvents scales approximately as $d \sim (\phi/T)^{1/3}$, where T is the temperature.^{3,4} This exponent for the concentration dependence is in good agreement with the self-consistent mean-field calculations of Whitmore and Noolandi.¹⁵ In contrast, a decrease of domain spacing with increasing concentration, $d \sim \phi^{-0.12}$, has been predicted for disordered semidilute solutions of block copolymers in a nonselective good solvent.^{16,17} Experimentally, an exponent of 0.05 has been reported for PS-PMMA diblocks in this regime.⁸ Shibayama et al. reported a scaling of $d \sim \phi^{-1/3}$ for semidilute PS-PB spherical micelles in the selective solvent tetradecane.¹⁸

The temperature dependence of micelle dimensions in block copolymer solutions has also been studied, for example, by Mortensen and Pedersen. They found that the core radius of micelles formed by a poly(ethylene oxide)-poly(propylene oxide)-poly(ethylene oxide) (EPE) triblock copolymer in aqueous solutions, spanning the dilute-concentrated regimes, increases with temperature.⁷ In contrast to the styrene-isoprene system considered here, where the solvent quality improves as the temperature is increased, in the EPE triblock the water solvation shell around the polymer becomes more disordered when the temperature is increased, and therefore the solvent is not as good as at low temperatures; thus, micelles are formed upon heating. Aqueous EPE solutions show an interesting array of phases,^{6,7} some of which are similar to those reported here, once the inverted temperature dependence is taken into account.

Recently, we reported an extensive series of measurements on styrene-isoprene (SI) copolymers in the slightly selective solvent di-*n*-butyl phthalate.¹⁰ The copolymers were an asymmetric SI diblock, with $M_w = 6 \times 10^4$ and $f_{PS} = 0.17$ by weight and the matching SIS triblock with $M_w = 1.2 \times 10^5$ and the same composition. The solvent is good for PS but was found to be a Θ solvent for PI near 80 °C. Solutions with polymer volume fractions, ϕ , near 0.20 were examined by rheology, flow birefringence, SAXS, and SANS. The results indicated that below 10 °C, the copolymers formed micelles with PI-rich cores. Interestingly, these micelles were elongated, with fits to model micellar form factors giving an aspect ratio of about 3. Upon increasing temperature, the micelles began to swell as solvent entered the core, leading to substantial intermicellar interactions. This was indicated by, for example, a 2-order-of-magnitude increase in the solution viscosity. The solutions then underwent an abrupt disordering transition near 43 °C. As temperature was further increased, the solution viscosity decreased but did not reach the level associated with a disordered, entangled solution of chains until 60–80 °C; this behavior was attributed to the progressive dissolution of the micelles, with experimental signatures reminiscent of the substantial concentration fluctuations reported for block copolymer melts and solutions. In this paper we describe SAXS and rheological measurements on the same copolymers, and over a similar temperature range, but with solution volume fractions ranging from 0.10 to 0.40. The micelles are found to pack on a hexagonal

lattice for $0.2 \leq \phi \leq 0.3$, before disordering at temperatures near 40 °C (diblock) or 50 °C (triblock); the ordered state is characterized by a solidlike viscoelastic response ($G' \geq G''$ at low frequencies). For $\phi > 0.3$ there is evidence of a lamellar phase, whereas for $\phi < 0.2$, only a viscosity maximum is evident, and $G' > G''$.

Experimental Section

Samples and Solutions. A poly(styrene-*b*-isoprene-*b*-styrene) triblock, and the matching poly(styrene-*b*-isoprene) diblock, were provided by D. Handlin (Shell Development Co.). The nominal block molecular weights were 1×10^4 , 1×10^5 , and 1×10^4 for the triblock and 1×10^4 and 5×10^4 for the diblock, with polydispersities of less than 1.06. The samples were thus designated SIS-120 and SI-60 and used without further treatment. The solvent, di-*n*-butyl phthalate (DBP), was obtained from Aldrich. It was washed with a 5% aqueous solution of NaHSO₃ followed by distilled water, dried over CaCl₂, and vacuum-distilled prior to use. Solutions were prepared gravimetrically, with the aid of methylene chloride as a cosolvent. The methylene chloride was stripped off under vacuum, at room temperature, until constant weight was achieved. The antioxidant 2,6-di-*tert*-butyl-4-methylphenol was added to each solution (0.3 wt % of polymer). Diblock and triblock solutions with volume fractions $\phi = 0.10, 0.14, 0.18, 0.20, 0.25$, and 0.30 , and $\phi = 0.36$ and 0.41 for the triblock, were prepared. The volume fractions were calculated from the weight fractions by assuming additivity of volumes and densities of 1.05, 0.913, and 1.043 g/mL for PS, PI, and DBP, respectively.

Rheology. Measurements were taken in a Rheometrics Fluids spectrometer (RFS II) using the cone and plate geometry (25 mm diameter, 4° cone angle, 200 μ m initial gap). Strain amplitudes, γ , ranged from 0.01 to 0.10 depending on concentration and temperature, such that measurements were all in the linear viscoelastic limit. Shear frequencies, ω , ranged from 0.01 to 100 rad/s and the temperature was controlled to within ± 0.2 °C.

Small-Angle X-ray Scattering. Small-angle X-ray scattering (SAXS) experiments were performed on beamlines 2.1 and 8.2 of the Synchrotron Radiation Source (SRS) at the Daresbury Laboratory, Warrington, U.K. Details of the storage ring, radiation, camera geometry, and data collection electronics have been given elsewhere.¹⁹

On station 2.1, white radiation from the source is monochromated using a bent triangular Ge(111) monochromator to give a high-intensity fixed wavelength beam of $\lambda = 1.54$ Å X-rays. Focusing is achieved in both horizontal and vertical directions by means of the monochromator and a quartz plane mirror, respectively. A 6 m camera was employed for this work, which gives a q range from 0.005 to 0.13 Å⁻¹. On station 8.2, white radiation from the source is monochromated using a cylindrically bent Ge(111) crystal to give an intense beam with $\lambda = 1.50$ Å. A vacuum chamber is placed between the sample and detectors to reduce air scattering and absorption. A 3 m sample-detector distance was used for this work on station 8.2.

On both stations, SAXS detectors that measure intensity in the radial direction (over an opening angle of 70° and an active length of 0.2 m) were used. These are only suitable for isomorphous scatterers. The active area increases radially, improving the signal-to-noise ratio at larger angles compared to single wire detectors. The spatial resolution of the SAXS detector is 500 μ m, and it can handle up to ~ 250 000 counts s⁻¹.

The samples for SAXS were prepared by inserting sealed glass capillaries in a Linkam hot stage mounted on an optical bench. The silver heating block of the hot stage contains a 4×1 mm tapered slot, which allows the transmitted and scattered X-rays to pass through unhindered. Cooling was achieved using a Linkam nitrogen flow controller, which also enables control of the heating rate, here set at 1, 2, or 3 °C/

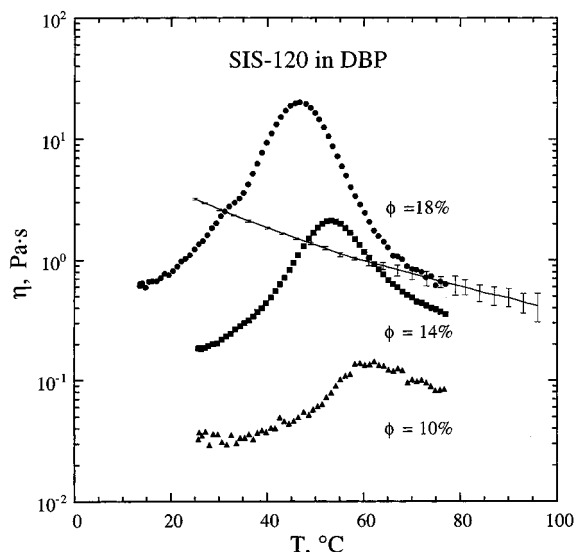


Figure 1. Temperature dependence of the viscosity for SIS-120 solutions with concentrations $\phi < 0.2$. The smooth curve represents the viscosity of an SIS-120 solution ($\phi = 0.18$) in dioctyl phthalate (corrected for the temperature-dependent differences in solvent viscosity).

min. Temperatures were recorded using a Linkam temperature controller.

A scattering pattern from an oriented specimen of wet collagen (rat-tail tendon) was used to calibrate the detector. A parallel plate ionization detector placed before the sample cell recorded the incident intensities. The experimental data were corrected for sample absorption and the positional alinearity of the detectors. The data are presented as a function of $q = 4\pi(\sin \theta)/\lambda$, where 2θ is the scattering angle and λ is the X-ray wavelength. Additional measurements were made on a SAXS instrument at the University of Minnesota. A Rigaku RU-200BVH rotating anode X-ray generator provided Cu K_α radiation ($\lambda = 1.54 \text{ \AA}$) from a $0.2 \times 2 \text{ mm}$ microfocus cathode; Franks mirror optics and a Siemens area detector were employed.

Results

The presentation of the scattering and rheology results is organized in the following fashion. First, we consider concentrations with $\phi \leq 0.18$, for which the micelles exhibit both "gaslike" and "liquidlike" behavior. Then the results for $0.20 \leq \phi \leq 0.41$ will be described. In this regime there is a distinct "solidlike" phase of micelles arranged on a lattice, which melts abruptly at an order-disorder transition (ODT). The ODT temperature is essentially independent of concentration, indicating its origin in solvent selectivity rather than styrene-isoprene interactions. We then compare the features of this ODT, and possible order-order transitions (OOTs), with results on block copolymer melts and neutral solvent solutions. The results are combined to provide a rather rich phase diagram for this system.

Solutions with $\phi \leq 0.18$. For the lower concentration triblock solutions studied, $\phi = 0.10, 0.14$, and 0.18 , rheological measurements revealed liquidlike behavior ($G' > G''$ at low frequencies) across the temperature range studied, and a maximum in the viscosity, $\eta(T)$, on increasing T , as shown in Figure 1. The increase in η is attributed to subtle changes in micelle size and shape with increasing solubility of the DBP in the PI-rich core, resulting in substantial crowding of the micellar solution. Thus, this transition can be viewed as a gradual progression from an isolated micelle

("gaslike") regime to a correlated-but-not-ordered ("liquidlike") regime. Using micellar dimensions obtained from form factor fits,^{10,20} it is possible to estimate the volume fraction of micelles in these solutions near the viscosity maximum. The solution volume fractions occupied by the micelles (core plus corona) are roughly 0.27, 0.20, and 0.15, for $\phi = 0.18, 0.14$, and 0.10 , respectively. Using results for the viscosity of suspensions of hard spheres,²¹ these apparent micellar volume fractions cannot account for the magnitude of viscosity enhancement observed in Figure 1. Consequently, one must conclude that intermicellar interactions are responsible. The decrease in η on the high T side of the maximum is attributed to the gradual dissolution of the micelles; it is helpful to recall that the critical micelle temperature (CMT) for this polymer in very dilute solution ($\phi = 0.002$) is $49 \text{ }^\circ\text{C}$.¹⁰ A curve depicting the temperature dependence of the viscosity for SIS-120 in DOP with $\phi = 0.18$ is shown for comparison; as DOP is a neutral solvent, this represents a disordered solution (the data have been corrected for the temperature-dependent difference in solvent viscosities). These data indicate that, at least from a rheological perspective, the DBP solution is disordered above about $70 \text{ }^\circ\text{C}$. The peak in η moves to lower T and becomes more pronounced with increasing ϕ as the intermicellar interactions become stronger. We do not interpret this movement as indicating a higher CMT for the lower ϕ solutions, but rather simply the diminished crowding at lower ϕ leading to a weaker maximum in η .

For the more dilute solutions with $\phi = 0.10$ and $\phi = 0.14$, the SAXS profiles do not exhibit any structure factor peaks. Instead, only form factor oscillations from a "gaslike" phase of micelles are observed. Consistent with the rheological data, this shows that the micelles are not positionally ordered for either diblock or triblock solutions at these concentrations. Figure 2 shows the T dependence of the form factor for SI-60 and SIS-120 with $\phi = 0.14$, upon heating from -30 to $+15 \text{ }^\circ\text{C}$. It should be noted that the cutoff evident at low q in this figure, and in all subsequent SAXS plots, is due to the beamstop. For the diblock, the form factor oscillations become weaker at higher T , and the location of each maximum moves to larger q . The oscillations are more pronounced for the $\phi = 0.14$ solution than for the $\phi = 0.10$ solution (not shown), as the micellar structure becomes better defined. In contrast, the form factor for the triblock is a weaker function of T and also does not change appreciably between the two concentrations considered here. The triblock micelle dimensions may be stabilized by PI "bridges" linking two coronal PS chains on opposite sides of the micelle. However, in general, the measurements for the two copolymers exhibit more features in common than sharp differences.

SAXS data for solutions with $\phi = 0.18$, taken during a heating ramp from -35 to $+80 \text{ }^\circ\text{C}$ at $3 \text{ }^\circ\text{C/min}$, are shown in Figure 3. For the diblock (Figure 3a), there is no structure factor peak at low T ; but oscillations can be observed in the high- q portion of the data, arising from the form factor of isolated micelles. Above about $10 \text{ }^\circ\text{C}$, however, a structure factor peak appears at low q , signaling the onset of significant intermicellar correlations. At the same time, the form factor oscillations diminish. A discontinuity in the T dependence of the intensity of the structure factor peak, $I(q^*)$, occurs close to $40 \text{ }^\circ\text{C}$, which is also near the maximum in η for the diblock in DBP.¹⁰ This signals the first evidence of an

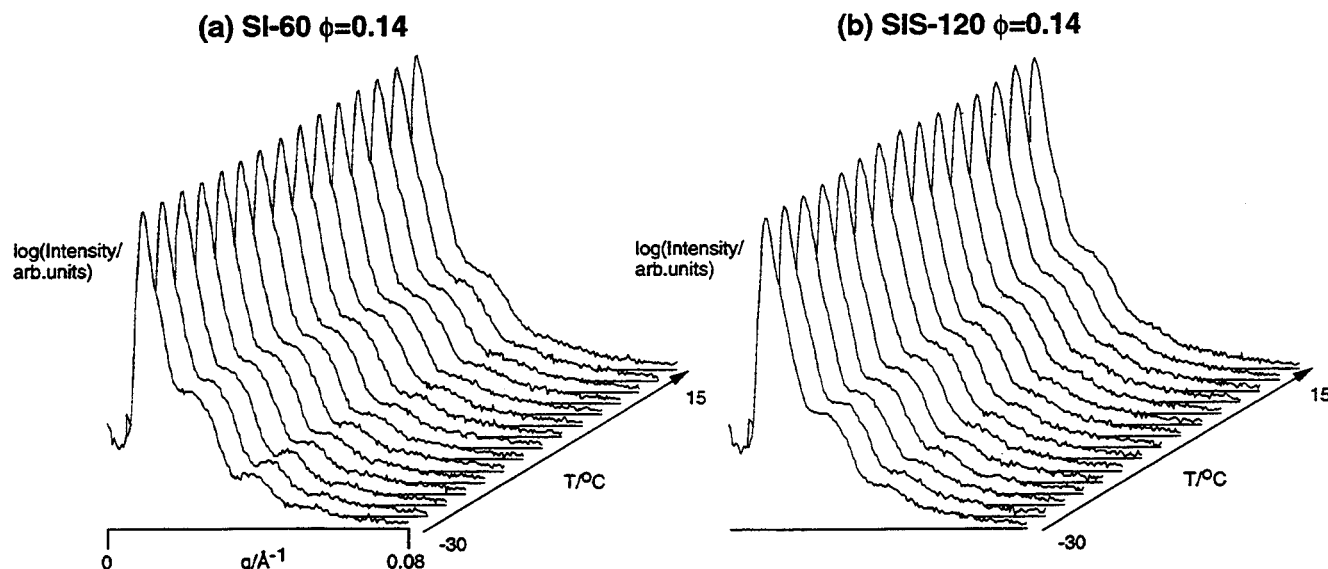


Figure 2. Temperature dependence of SAXS profiles for $\phi = 0.14$ solutions in DBP: (a) SI-60; (b) SIS-120.

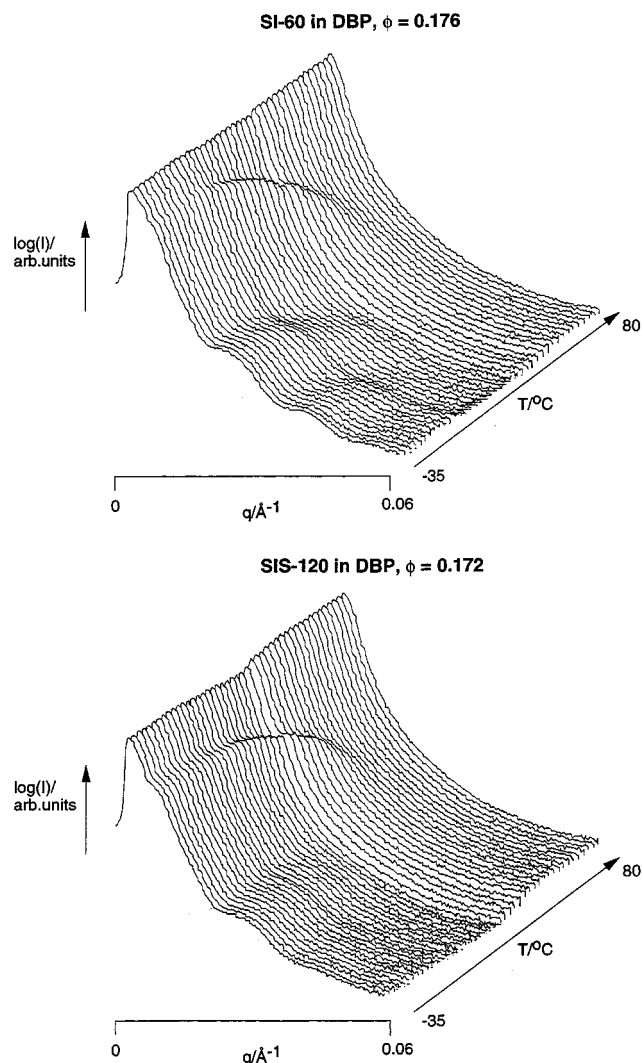


Figure 3. Temperature dependence of SAXS profiles for $\phi = 0.18$ solutions in DBP: (a) SI-60; (b) SIS-120.

ODT, as will be discussed in more detail subsequently. At still higher T the intensity of the structure factor peak decreases until it disappears, and we associate this with the breaking-up of micelles as the diblock chains dissolve in solution at higher T . The SAXS data for the

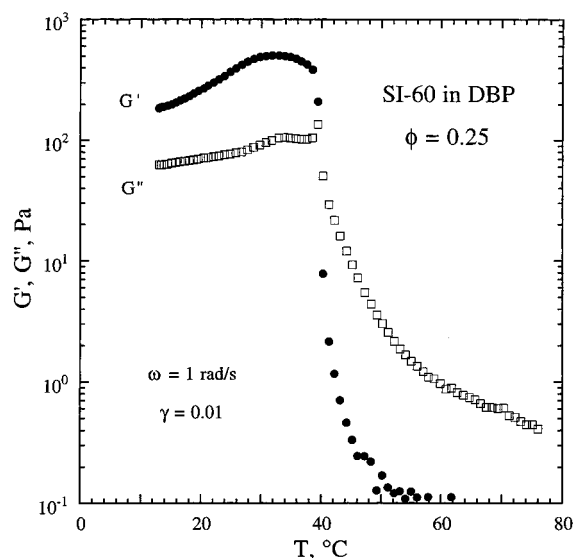


Figure 4. Dynamic shear moduli measured at 1 rad/s and 1% strain amplitude as a function of temperature for the $\phi = 0.25$ SI-60 solution.

corresponding triblock solution are presented in Figure 3b and are qualitatively similar to those for the diblock solution in Figure 3a. However, in contrast to the diblock, a shoulder anticipating the structure factor peak is observed even at the lowest T . The ODT is again suggested by a discontinuity in the T dependence of $I(q^*)$ near 40 °C, and the peak progressively disappears at higher T .

Solutions with $\phi \geq 0.20$. Rheological measurements reveal that, in contrast to the lower concentration solutions, solutions with $\phi \geq 0.2$ are characterized by $G' > G''$, below an ODT that is evident from a discontinuous decrease in the dynamic elastic moduli as a function of temperature measured at a fixed low frequency. This was demonstrated in the previous paper for $\phi = 0.20$ ¹⁰ and is illustrated by the representative data for the $\phi = 0.25$ SI-60 solution shown in Figure 4, which indicate an ODT at 39 °C (upon heating). The frequency dependence of the moduli at representative temperatures well above the ODT confirm that the solution behaves as a liquid, with the characteristic terminal regime scaling. In contrast, for $T < 39$ °C, G'

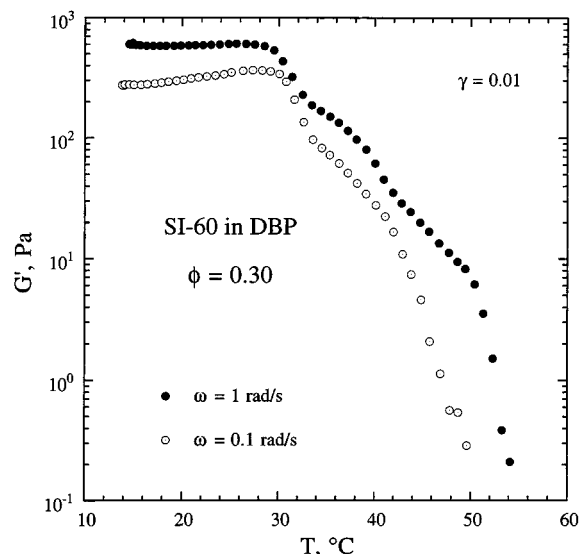


Figure 5. Dynamic elastic storage modulus measured at 0.1 and 1 rad/s (1% strain amplitude) as a function of temperature for the $\phi = 0.30$ SI-60 solution.

$> G''$ and the response is clearly that of an ordered, solidlike structure. The abrupt drop in the moduli at the ODT is similar in character to that seen in melt block copolymers,²² but the magnitude of the drop (a factor of over 1000 in G') is remarkable. For the $\phi = 0.30$ solution in Figure 5, the ODT is less readily located as at least two features are apparent in $G'(T)$. However, we tentatively assign the ODT to approximately 43 °C, based on the rheological measurements at the lower frequency (0.1 rad/s) shown (the lower frequency response is more sensitive to microstructure and is preferred as a diagnostic of the ODT). Measurements of the isochronal dynamic elastic moduli as a function of T suggest that some kind of order–order transition (OOT), or change in micellar packing, occurs at 31 °C (see Figure 5). It is conceivable that the small local maxima in the dynamic moduli near 33 °C in Figure 4 are also precursors for the same OOT. The scattering experiments discussed below also give evidence of this change but do not indicate a clear change in symmetry.

Extensive rheological measurements were performed on the triblock solutions, as for the diblocks, and isochronal measurements of $G'(T)$ for solutions of SIS-120 with $\phi \geq 0.2$ are presented in Figure 6. These data clearly show that in solutions with $\phi = 0.20, 0.25$, and 0.30 an ODT occurs at 47–48 °C, although the transition is noticeably less abrupt for the highest of these three concentrations. Although there is no evidence of a possible OOT in G' , traces for G'' consistently indicate a maximum near 33 °C, as for the diblock solutions. Measurements on the triblock were extended to $\phi = 0.41$, as shown in Figure 7. The dynamic moduli at this concentration are substantially larger than those for the lower concentration solutions at a given low temperature, following the trend shown in Figure 6 where G' increases monotonically with ϕ in the ordered state. The frequency dependence of G' for the $\phi = 0.41$ solution at various temperatures above and below the ODT are presented in Figure 8. At 76 and 95 °C the low-frequency response is liquidlike, whereas at 20 and 38 °C, an ordered structure is indicated by the nonterminal response of the moduli and the fact that $G' > G''$.

SAXS data for the diblock solution with $\phi = 0.25$ taken during a heating ramp from 25 to 60 °C are

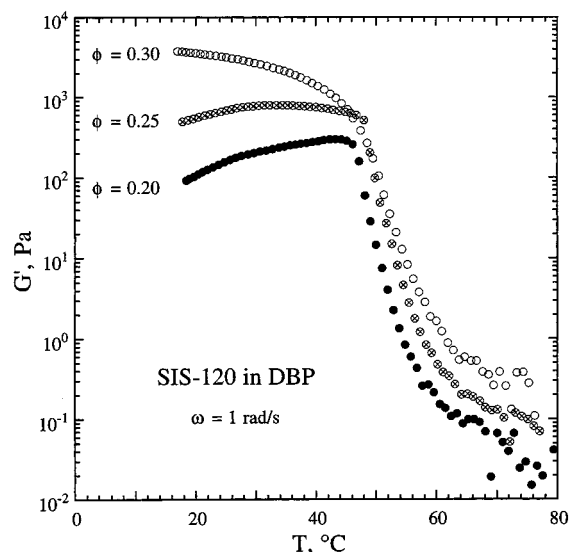


Figure 6. Temperature dependence of the dynamic storage modulus ($\omega = 1$ rad/s) for three SIS-120 solutions.

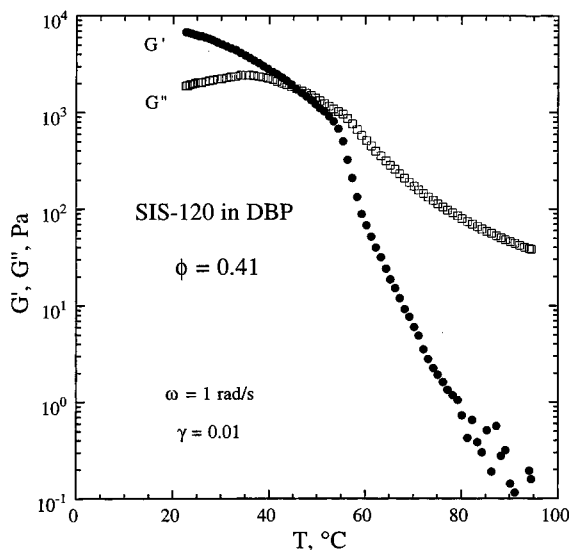


Figure 7. Temperature dependence of the isochronal dynamic shear moduli ($\omega = 1$ rad/s) for the $\phi = 0.41$ SIS-120 solution.

presented in Figure 9a. The presence of higher order reflections shows that this solution forms an ordered phase up to the order–disorder transition at 42 °C. In Figure 9b, the lowest temperature traces from Figure 9a are averaged and plotted as I vs q . Denoting the peak position of the principal reflection as q^* , higher order reflections are observed at approximately $\sqrt{4}q^*$ and $\sqrt{7}q^*$. This is consistent with a hexagonal morphology, although the expected $\sqrt{3}q^*$ reflection is rather weak. A hexagonal structure is natural given that the micelles are elongated, as shown by modeling of the form factor data for the $\phi = 0.20$ solutions and the observation of optical birefringence and shear alignment in this phase.¹⁰ Similar behavior is observed for the $\phi = 0.30$ solution, except that analysis of the peak intensity as a function of temperature (to be presented subsequently) also suggests that a structural transition may occur prior to the ODT in this sample.

SAXS results for solutions of the triblock copolymer over the concentration range from 0.2 to 0.3 resemble those from the corresponding diblock solutions. However, at higher concentrations the SAXS results indicate

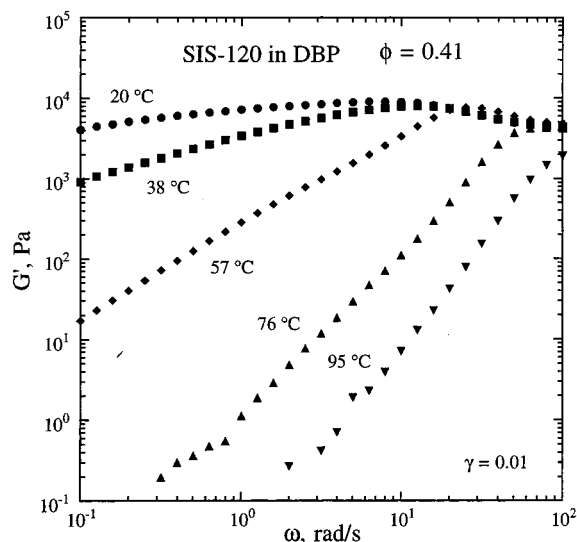


Figure 8. Frequency sweeps of the dynamic elastic modulus for the $\phi = 0.41$ SIS-120 solution at temperatures spanning the ODT.

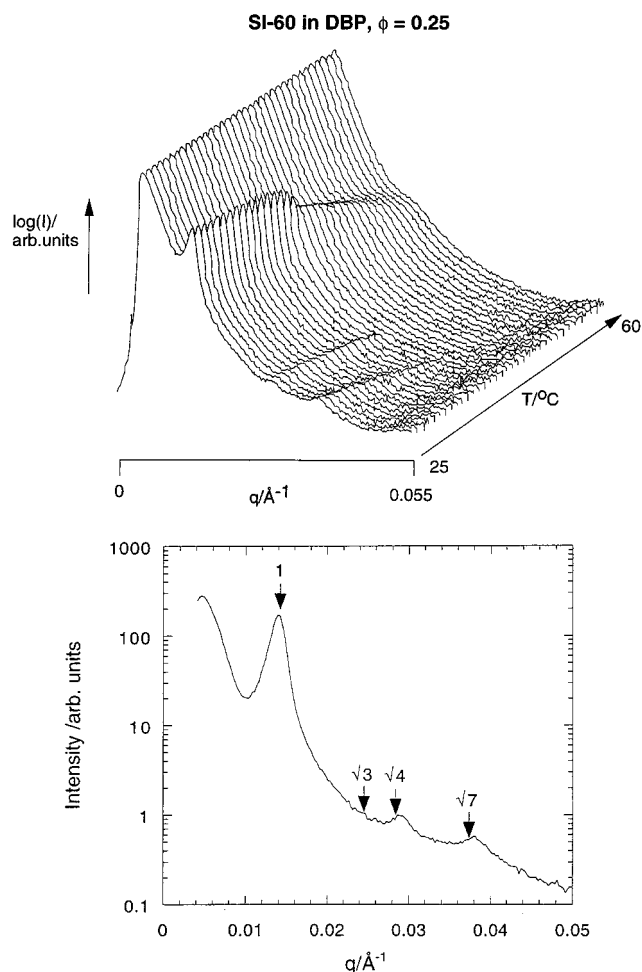


Figure 9. SAXS profiles for SI-60, $\phi = 0.25$: (a) temperature dependence; (b) low-temperature q dependence.

a change in morphology. Form factor oscillations are not observed for the $\phi = 0.41$ solution on heating from 25 to 80 °C, as shown in Figure 10a. Rather, the pronounced structure factor peak at low q is supplemented by a very weak additional reflection at $3q^*$. Measurements on a laboratory SAXS camera on a solution with $\phi = 0.36$ give clear evidence of isotropic

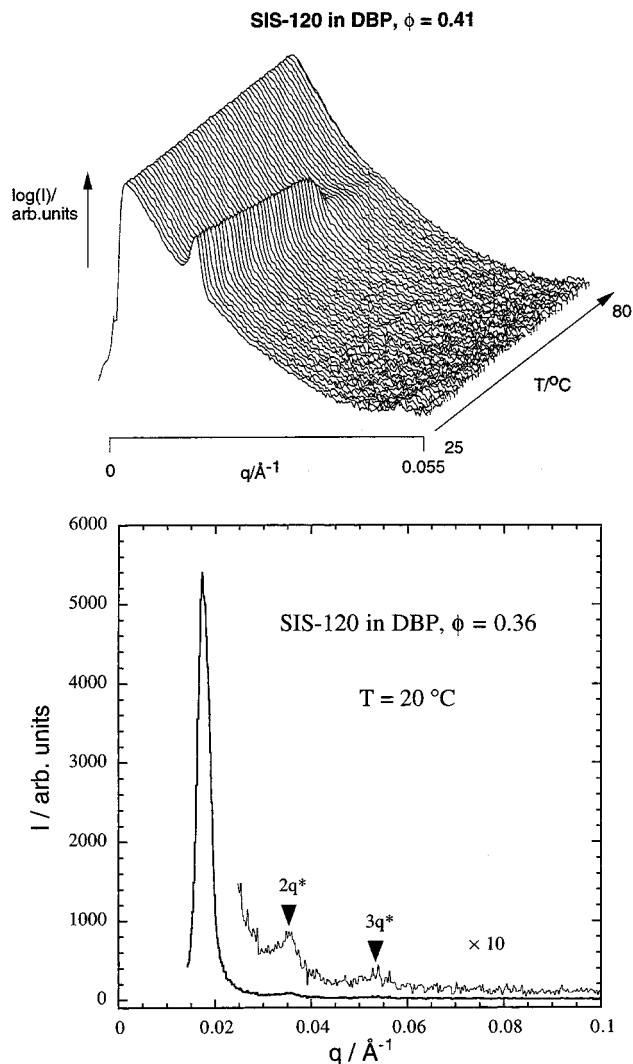


Figure 10. SAXS profiles for SIS-120 solutions in DBP: (a) $\phi = 0.41$; (b) $\phi = 0.36$.

scattering with peaks at q^* , $2q^*$, and $3q^*$, as shown in Figure 10b. Consequently, we infer that solutions in this concentration regime adopt a lamellar morphology. The low-temperature melt morphology of both SI-60 and SIS-120 is hexagonally packed cylinders (as confirmed by SAXS and TEM experiments), where PS forms the cylinders; in the melt both samples also transform to a cubic array of spheres just prior to the ODT.^{23,24} This means that as the concentration of the solution is increased, a crossover must occur between a hexagonal phase of ellipsoidal micelles with PI cores, formed as a result of solvent selectivity, and a hexagonal phase of PS cylinders formed in the melt due to the composition of the block copolymer. A lamellar phase is the natural intermediate, although one might also anticipate possible windows of bicontinuous cubic structures between lamellar and hexagonal phases.^{25,26} All traces of the reflection at $3q^*$ in Figure 10a disappear at the ODT (52 °C), which is also well-defined for this solution.

Phase Diagram. In general, the SAXS and rheological results are in very good agreement, in terms of locating the various transitions; the results are summarized in Tables 1 (SI-60) and 2 (SIS-120). Throughout, the behavior of the diblock and the triblock are very similar, except for rather subtle features. The SAXS and rheological results are combined in Figure 11 into an approximate "phase diagram" for the PS-PI/DBP sys-

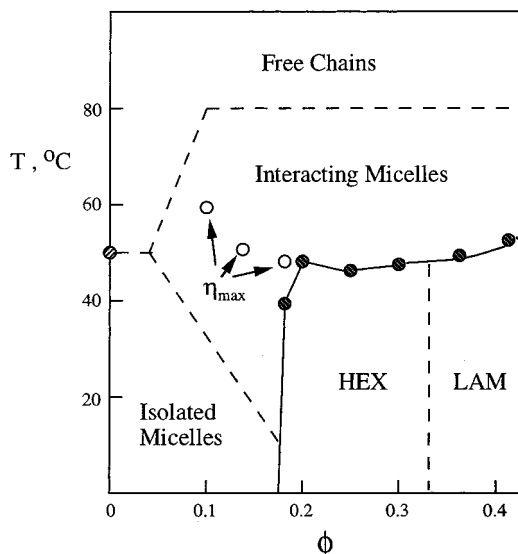


Figure 11. Phase diagram for SIS-120 solutions in DBP.

tem; individual ODTs are noted as filled symbols. For the concentration range $0 \leq \phi \leq 0.4$, five regimes of behavior are delineated. At high temperatures, $T \geq 80$ °C, the solutions are disordered at all concentrations. In this regime DBP becomes a sufficiently good solvent for the PI block to suppress micelle formation. For semidilute and concentrated solutions, there is then a regime of interacting micelles extending over a range of perhaps 30 °C, in which the SAXS and rheological properties are reminiscent of those in the corresponding regime for block copolymer melts: $I(q^*)^{-1}$ does not scale linearly with T^{-1} , and the viscosity is higher than for a disordered solution. This temperature window corresponds roughly to the interval between the dilute solution CMT and the critical temperature for PI/DBP solutions. At lower T , four regimes of behavior are resolved, depending on concentration. Beginning with very dilute solutions, these are a "gaslike" phase of isolated micelles, a "liquidlike" phase of interacting micelles, and two "solidlike" phases, with hexagonal and lamellar symmetry. The hexagonal phase in Figure 11 has PI in the "cylindrical" domains, whereas the melt morphology has PS cylinders, and the intermediate lamellar phase is the expected compromise between the competing curvatures (solvent-selectivity-induced versus copolymer-composition-induced, respectively). Such a progression is not unusual in small molecule amphiphile systems.²⁵ The melting of the solid phases occurs at temperatures that are all roughly the same and close to the CMT in dilute solutions, indicating that there is a "critical" degree of solvent selectivity necessary to produce block segregation that is almost independent of concentration. Four final comments about the phase diagram in Figure 11: (i) it is developed on the basis of the triblock data, but the diblock results would give essentially the same features and approximate locations; (ii) other features not yet observed are certainly possible, such as regions of two-phase coexistence, or even bicontinuous structures, intermediate between lamellar and hexagonal microstructures; (iii) the possible order–order transitions are not indicated; (iv) the results are all a direct consequence of solvent selectivity. In the more neutral solvents toluene and dioctyl phthalate, this region of the phase diagram would be entirely disordered for both copolymers; the ODTs in toluene, for example, are located above $\phi =$

0.5 for the triblock and $\phi = 0.6$ for the diblock at room temperature.²³

Peak Intensity and Position. For block copolymer solutions in a nonselective good solvent the inverse structure factor is given by^{16,17}

$$S(q)^{-1} = (2\phi/IN)\{F(q) - 2\chi^*N\} \quad (1)$$

Here l is a segment length for the block copolymer and $F(q)$ is a function of the radius of gyration and composition of the block copolymer. The effective interaction parameter in semidilute solution is $\chi^*N = \chi_{AB}N\phi^{(1+z)/(3\nu-1)}$, where ν is the Flory exponent ($\nu = 0.59$ in good solvents) and $z = 0.22$.^{10,11} The function $F(q)$ has a minimum, and hence $I(q)^{-1}$ has a maximum, at $q = q^*$, which is independent of χ and thus of temperature. Empirically, χ is found to be inversely proportional to temperature

$$\chi = A + B/T \quad (2)$$

where A and B are constants; thus $I(q^*)$ is predicted to change linearly with $1/T$.

The data on heating for the diblock solutions clearly show a break in the inverse intensity at the same temperature, which we identify as the order–disorder transition (ODT). For the $\phi = 0.20$ solution, the SAXS ODT is determined to be 36 ± 1 °C, as reported previously.¹⁰ The SAXS value for the ODT is in excellent agreement with the value from rheology, 36 °C. The ODT temperature is reproducible on successive heating ramps, although there is significant hysteresis associated with a given heat/cool cycle. The nonlinearity in $1/I(q^*)$ versus T^{-1} at high temperatures is indicative of the presence of block copolymer compositional fluctuations.²⁷ Features in $1/I(q^*)$ and the slope of q^* occur at an ODT of 42 ± 1 °C for the $\phi = 0.25$ solution, as shown in Figure 12a. For the $\phi = 0.30$ solution, the ODT is assigned in Figure 12b at 42.5 ± 1 °C, to be in agreement with the value from rheology. The features at 31 and 37.5 °C are apparently indicative of changes in packing, not the ODT, because the frequency dependence of the dynamic moduli at 38 °C shows clear nonterminal behavior; i.e., the solution is still ordered at this temperature. The weak feature in $1/I(q^*)$ at 31 °C occurs at the same temperature as a sharp drop in the isochronal dynamic elastic storage modulus, shown in Figure 5.

As reported previously, sharp discontinuities in $1/I(q^*)$ and q^* are observed on heating the $\phi = 0.20$ triblock solution at 50 ± 1 °C, which is the ODT for this concentration, in good agreement with rheology.¹⁰ Although there is a significant hysteresis associated with this transition (during a cooling ramp at 1 °C/min discontinuities in the slopes of q^* and $1/I(q^*)$ were not observed), this value is reproduced on subsequent heating runs (performed 2 h later and 5 months later), as were the discontinuities. For the $\phi = 0.25$ solution, the ODT is located at 43 ± 1 °C, whereas for the most concentrated solution, the ODT occurs at 52 ± 1 °C. The data (not shown) do not extend to sufficiently low temperatures to determine if any order–order phase transition precedes the ODT in these solutions.

We have also considered the scaling of q^* with solution concentration. A reference temperature $T = 35$ °C just below the ODT for all solutions was chosen, and the results are shown in Figure 13. It is immediately clear that q^* is a strong function of concentration, with an approximate scaling of $\phi^{1/3}$. There is

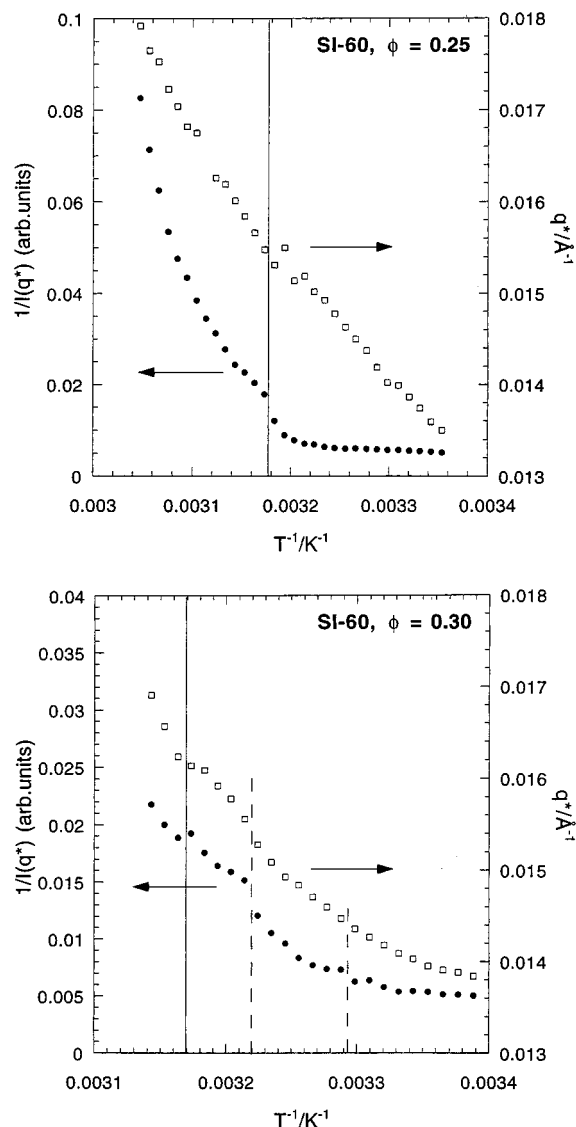


Figure 12. SAXS peak position, q^* , and inverse peak intensity as a function of inverse temperature for SI-60: (a) $\phi = 0.25$; (b) $\phi = 0.30$. The vertical lines indicate the assigned ODTs, and dashed lines possible OOTs.

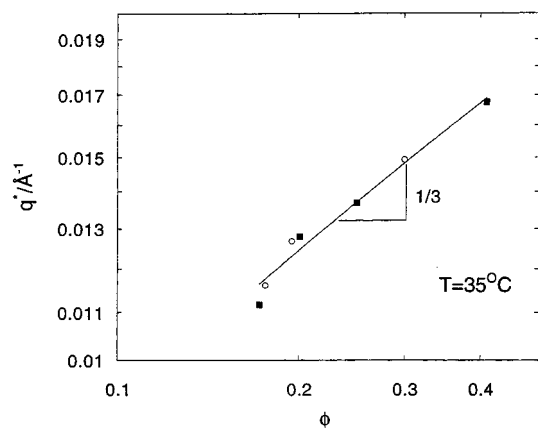


Figure 13. SAXS peak position at a reference temperature $T = 35\text{ }^{\circ}\text{C}$ as a function of concentration for diblock (○) and triblock (■) copolymer solutions.

some indication that the dependence is stronger at concentrations below the onset of order, i.e., $\phi \leq 0.2$. For symmetric SI copolymers in neutral solvents, Hashimoto and co-workers found that q^* scales as $\phi^{-1/3}$ in

Table 1. Transitions in SI-60/DBP Solutions

ϕ	SAXS	rheology
0.10	liquid of micelles	N/A
0.14	liquid of micelles	N/A
0.18	ODT = 40 °C (heating at 3 °C/min)	N/A
0.20 ^a	ODT = 36 °C (heating at 3 °C/min)	ODT = 36 °C
0.25	ODT = 42 °C (heating at 1 °C/min)	ODT = 39 °C (heating at 0.4 °C/min)
0.30	features at 31, 37, and 43 °C (heating at 1 °C/min)	features at 31 and 43 °C ($w = 0.1\text{ rad/s}$), 31 °C and 50 °C ($w = 1\text{ rad/s}$)

^a Results for this sample were presented previously.¹⁰

Table 2. Transitions in SIS-120/DBP Solutions

ϕ	SAXS	rheology
0.10	liquid of micelles	max. viscosity at 59 °C
0.14	liquid of micelles	max. viscosity at 53 °C
0.18	ODT = 39 °C (heating at 3 °C/min)	max. viscosity at 47 °C
0.20 ^a	ODT = 50 °C (heating at 3 °C/min)	ODT = 47 °C (heating at 0.4 °C/min)
0.25	ODT = 43 °C (heating at 1 °C/min)	ODT = 48 °C (heating at 0.4 °C/min)
0.30	N/A	ODT = 48 °C (heating at 0.4 °C/min)
0.41	ODT = 52 °C	ODT = 54 °C heating at 0.4 °C/min

^a Results for this sample were presented previously.¹⁰

the concentrated regime ($\phi > 0.2$).^{3,4} This result is in agreement with self-consistent mean-field theory¹⁵ and reflects the increased stretching of the chains with increasing concentration, due to styrene–isoprene interactions. In contrast, we find an increase in q^* with concentration, attributable to solvent selectivity. The approximate exponent of 1/3 implies a uniform reduction of the domain spacing in all three spatial dimensions as concentration is increased. This, in turn, suggests that these micelles have a finite length, which is consistent with the form factor fits;^{10,20} if they were infinite cylinders a scaling of $d \sim \phi^{-1/2}$ would be obtained.²⁸ The same interpretation of this scaling has been given for the domain spacing obtained from SAXS for the hexagonal micellar phase of an amphiphile in aqueous solution.²⁹ A similar exponent and interpretation were reported by Shibayama et al. for PS–PB spherical micelles in the selective solvent tetradecane, but only for $\phi \leq 0.2$.¹⁸

Summary

SAXS and rheology have been used to investigate the state of order in concentrated solutions of matched styrene–isoprene di- and triblock copolymers. The solvent, DBP, is slightly selective for the styrene block, being a Θ solvent for polyisoprene near 80 °C. The rich phase behavior of these solutions over the range $0 \leq T \leq 100\text{ }^{\circ}\text{C}$ and $0 \leq \phi \leq 0.4$ is summarized in Figure 10, and the corresponding transitions are listed in Tables 1 and 2. At low temperatures the copolymers form ellipsoidal micelles for $\phi < 0.2$, and the micelles pack onto a hexagonal lattice for $\phi > 0.2$; at $\phi > 0.3$ there is evidence of a lamellar phase. With increasing temperature, the ordered solutions display a distinct ODT around 40–50 °C, and the disordered micellar solutions show a strong maximum in the viscosity. Above the ODT there is a significant range of temperature over which evidence of chain association persists, before the micelles are fully dissociated. The fact that the ODT

temperature is essentially independent of ϕ indicates that it is determined by solvent selectivity, not styrene–isoprene interactions. This is also consistent with the fact that neither copolymer is in the ordered state in a neutral good solvent over this range of ϕ .²³ At the higher concentrations, there is some indication in both SAXS and rheology of subtle changes in packing just prior to the ODT.

Acknowledgment. This work was supported in part by the National Science Foundation (Grants DMR-9018807 and 9528481 to T.P.L.) and the Center for Interfacial Engineering, an NSF-sponsored Engineering Research Center at the University of Minnesota. I.W.H. and T.P.L. are grateful to NATO for a Collaborative Research Grant (CRH/940078). I.W.H., A.J.R., and J.P.A.F. were supported by the Engineering and Physical Sciences Research Council (U.K.). We thank E. Towns-Andrews and D. Hajduk for assistance with the SAXS experiments at Daresbury and at Minnesota, respectively.

References and Notes

- (1) Tuzar, Z.; Kratochvil, P. In *Surface and Colloid Science*; Matijevic, E., Ed.; Plenum Press: New York, 1993; Vol. 15.
- (2) Watanabe, H.; Kotaka, T. *Polym. Eng. Rev.* **1984**, *4*, 73.
- (3) Hashimoto, T.; Shibayama, M.; Kawai, H. *Macromolecules* **1983**, *16*, 1093.
- (4) Shibayama, M.; Hashimoto, T.; Hasegawa, H.; Kawai, H. *Macromolecules* **1983**, *16*, 1427.
- (5) Brown, R. A.; Masters, A. J.; Price, C.; Yuan, X. F. In *Comprehensive Polymer Science*; Booth, C., Price, C., Eds.; Pergamon Press: Oxford, U.K., 1989; Vol. 2.
- (6) Mortensen, K. *Europhys. Lett.* **1992**, *19*, 599.
- (7) Mortensen, K.; Pedersen, J. S. *Macromolecules* **1993**, *26*, 805.
- (8) Mayes, A. M.; Barker, J. G.; Russell, T. P. *J. Chem. Phys.* **1994**, *101*, 5213.
- (9) Lodge, T. P.; Pan, C.; Jin, X.; Liu, Z.; Zhao, J.; Maurer, W. W.; Bates, F. S. *J. Polym. Sci., Polym. Phys. Ed.* **1995**, *33*, 2289.
- (10) Lodge, T. P.; Xu, X.; Ryu, C. Y.; Hamley, I. W.; Fairclough, J. P. A.; Ryan, A. J.; Pedersen, J. S. *Macromolecules* **1996**, *29*, 5955.
- (11) McConnell, G. A.; Gast, A. P. *Phys. Rev. E* **1996**, *54*, 5447.
- (12) Raspaud, E.; Lairez, D.; Adam, M.; Carton, J.-P. *Macromolecules* **1994**, *27*, 2956.
- (13) Bates, F. S.; Fredrickson, G. H. *Annu. Rev. Phys. Chem.* **1990**, *41*, 525.
- (14) Watanabe, H.; Kotaka, T. *Polym. J.* **1982**, *14*, 739.
- (15) Whitmore, M. D.; Noolandi, J. *J. Chem. Phys.* **1990**, *93*, 2946.
- (16) Fredrickson, G. H.; Leibler, L. *Macromolecules* **1989**, *22*, 1238.
- (17) Olvera de la Cruz, M. *J. Chem. Phys.* **1989**, *90*, 1995.
- (18) Shibayama, M.; Hashimoto, T.; Kawai, H. *Macromolecules* **1983**, *16*, 16.
- (19) Towns-Andrews, E.; Berry, A.; Bordas, J.; Mant, G. R.; Murray, P. K.; Roberts, K.; Sumner, I.; Worgan, J. S.; Lewis, R.; Gabriel, A. *Rev. Sci. Instrum.* **1989**, *60*, 2346.
- (20) Pedersen, J. S.; Hamley, I. W.; Lodge, T. P. Unpublished results.
- (21) Nielsen, L. E. *Polymer Rheology*; Marcel Dekker: New York, 1977.
- (22) Fredrickson, G. H.; Bates, F. S. *Annu. Rev. Mater. Sci.* **1996**, *26*, 503.
- (23) Lodge, T. P.; Blazey, M. A.; Liu, Z.; Hamley, I. W. *Macromol. Chem. Phys.* **1997**, *198*, 983.
- (24) Ryu, C. Y.; Lee, M. S.; Hajduk, D. A.; Lodge, T. P. *J. Polym. Sci., Polym. Phys. Ed.* **1997**, *35*, 2811.
- (25) Seddon, J. M. *Biochim. Biophys. Acta* **1990**, *1031*, 1.
- (26) Bates, F. S.; Schulz, M. F.; Khandpur, A. K.; Förster, S.; Rosedale, J. H.; Almdal, K.; Mortensen, K. *J. Chem. Soc., Faraday Discuss.* **1994**, *98*, 7.
- (27) Fredrickson, G. H.; Helfand, E. *J. Chem. Phys.* **1987**, *87*, 697.
- (28) Hentschke, R.; Taylor, M. P.; Herzfeld, J. *Phys. Rev. A* **1989**, *40*, 1678.
- (29) Amaral, L. Q.; Gulik, A.; Itri, R.; Mariani, P. *Phys. Rev. A* **1992**, *46*, 3548.

MA970831Y